Eur. Phys. J. B **37**, 433–438 (2004)
DOI: 10.1140/epjb/e2004-00078-0

THE EUROPEAN PHYSICAL JOURNAL B

Fragmentation of Si clusters studied by a dynamical Hartree-Fock method at semi-empirical level

A.M. Mazzone[a]

C.N.R., IMM, Via Gobetti 101, 40129 Bologna, Italy

Received 12 August 2003
Published online 9 April 2004 –

Abstract. This study describes fragmentation of silicon clusters of size $N \leq 40$. Fragmentation is produced by the increase of the kinetic energy E_k of the nuclear system and a time-dependent Hartree-Fock method, with a semi-empirical Hamiltonian is used for the evaluation of the transient ensuing the energy input. A typical channel of fragmentation has been observed which consists on the emission of small (from 1 to 5) groups of atoms. Due to these losses, the fragmentation remnants for $N \geq 20$ reach a size equal to 1/2–1/4 of the original one. These trends are in agreement with the experimental ones. Furthermore the critical energies obtained from fragmentation calculations are discussed in the light of the binding energies evaluated for the stationary state.

PACS. 21.60.-n Nuclear structure models and methods – 31.15.Ct Semi-empirical and empirical calculations (differential overlap, Hückel, PPP methods, etc.) – 79.60.Jv Interfaces; heterostructures; nanostructures

1 Introduction

In the field of clusters there is a considerable interest for the processes leading to fragmentation. The thrust of these studies is to find structures with new and unforeseen properties by mapping regions of the configurational space different from the stationary ones.

Much work has been devoted to silicon clusters. In fact, silicon is of particular importance for the microelectronic industry and therefore a detailed knowledge of the physical and chemical properties of the clustered state of this material is highly desirable. In addition, silicon clusters seem to hold significant potentialities for photoluminescent and quantum devices and therefore the effort in this field is intensive. Studies on fragmentation of silicon cluster ions with a size in the range 10–100 showed the emission of large fragments well above the monomer size [1–5]. At variance with it, evaporation of monomers and dimers has been recently reported for nanometric clusters [6].

This difference raises an important question. Are the fragments observed at small size the components of the cluster ground state or are due to the reaggregation of monomers and dimers produced upon fragmentation? The traditional interpretation (see [7,8] and the references therein) is that the fragments are subunits of the cluster structure and therefore fragmentation is a fundamental tool to investigate structural properties of clusters. However studies on cluster melting invariably show that even a modest energy input leads to a complex structural evolution where the memory of the initial state is rapidly lost. Obviously, the rigorous solution of this problem requires the evaluation of the entire fragmentation transient. In spite of the development of very efficient ab initio and DFT calculations, the evaluation of time-dependent effects is still a major computational problem. In this study, which complements previous studies on fragmentation of clusters formed by lead and tin [9], fragmentation is considered from both a physical and a methodological standpoint. On one side, in fact, we attempt to gain insight on the process of fragmentation by its direct simulation. The study of the cluster evolution during the fragmentation transient allows the assessment of the structure of fragments and of the energy needed for fragmentation. On the other side, the functional dependence of this energy on the cluster size is compared with the binding energies of the ground state, which are commonly believed to represent accurate indicators of the cluster stability. This represents the methodological aspect of the study.

The paper is organized as follows. Section 2 describes the equations governing the dynamical evolution and the fragmentation conditions. Section 3 illustrates the properties of the ground state obtained from the minimization of the total energy. In this paragraph a brief comparison with other theories and with experiments is also made. The dynamics of fragmentation is shown in Section 4.

2 Computational details

In fragmentation studies either a classical representation or quantum mechanical methods (QM) are used. The

[a] e-mail: mazzone@bo.imm.cnr.it

classical approach, based on statistical methods or on molecular dynamics, is the one more commonly adopted and has been widely applied to clusters of rare-gas and noble metal atoms and fullerenes up to the size $N \sim 60$ (attained for argon clusters and fullerenes [11]). Generally, QM are mixed schemes combining classical mechanics for the nuclei with a quantum mechanical treatment for the electrons. Owing to their great complexity, these methods appear to be at a formative stage and have been generally used for simple elements or small clusters (a detailed list of references on experiments on cluster fragmentation and melting and on the related theoretical approaches is reported in [9]).

It is thought that the implementation of a time-dependent QM method represents one of the methodological contribution of this work. The method has already been described in [9]. Here it is only recalled that it is based on the time-dependent Hartree-Fock formulation, as presented in [10], and the main assumptions of the calculations are as follows:

(i) the nuclear dynamics is described by classical dynamics,
(ii) a LCAO representation is used for the electron wavefunction. This wavefunction is evaluated under adiabatic assumptions at the end of the nuclear motions. In a one-dimensional notation the forces needed for nuclear dynamics are given

$$\partial E_{HF}/\partial X_i = \sum_{\mu\nu} P_{\mu\nu}(\partial H_{\mu\nu}/\partial X_i) + 1/2 \sum_{\mu\nu\lambda\sigma} P_{\mu\nu}P_{\lambda\sigma}(\partial/\partial X_i)(\mu\lambda|\nu\sigma) - \sum_{\mu\nu} W_{\mu\nu}(\partial S_{\mu\nu}/\partial X_i) + \partial V_{nuc}/\partial X_i \quad (1)$$

where μ, ν indicate electronic orbitals. The matrix element $H_{\mu\nu}$ is the one-electron Hamiltonian (kinetic and potential energy) due to the electrostatic field of the nuclei. $P_{\mu\nu}$, $S_{\mu\nu}$ and $W_{\mu\nu}$ are the element of the bond-order, density and energy matrix, respectively.

In time-dependent calculations the nuclear coordinates X_i are evaluated at each time step dt using equation (1). After this step, the electron wavefunction is constructed by the minimization of the HF energy in the cluster structure determined by the nuclear motions. This allows a new evaluation of $\partial E_{HF}/\partial X_i$ and hence a new cycle at $t + dt$.

The use of classical dynamics allows an unambiguous identification of the parameters of the nuclear dynamics. The displacements and the velocities of the atoms have their usual meaning, as in classical mechanics, and the cluster kinetic energy is given by $\sum_N MV_i^2/2$, where $V_i = \partial X_i/\partial t$, $i = 1, 2, 3$ are the Cartesian velocity components of the i atom.

The fragmentation conditions are taken from [12]. Each fragmentation event starts from the cluster ground state by applying the kinetic energy E_k to the entire cluster. Prior to fragmentation a normal mode analysis is carried out and the energy of each mode is scaled so as to obtain the wanted E_k for the whole cluster. The simulation is continued as a constant energy simulation for a duration of about 1000 fs. Generally, numerical errors are limited to the initial 50–100 fs during which a large overshoot of the potential energy may occur in response to the input kinetic energy. This effect is healed by the continuous rescaling of the time step dt and from approximately 150 fs on the error in the total energy conservation is below the sixth significant figure. These initialization errors are of no consequence on fragmentation. In fact, important structural modifications of the cluster shape start at approximately 200 fs from the beginning of the transient (see below).

The HF integrals in equation (1) are calculated at semiempirical level using the Modified Neglect of Diatomic Orbital scheme with AM1 parametrization using MOPAC software [13–15]. The AM1 parametrization is based on atomic and molecular data and it has been often compared with experiments in studies within the chemical literature. A recent analysis and discussion is presented in [16]. The use of this Hamiltonian represents a significant improvement over the original formulation [10] where a simple Neglect Differential Diatomic Overlap method was applied.

3 The cluster ground state. Binding and emission energies

To set the stage briefly, we recall some experimental and theoretical data on silicon clusters. The shape of clusters with size in the range 10 is now well assessed [17]. At $N \geq 4$ the clusters acquire a three-dimensional shape and grow by the accretion of capping terminations placed at the corners or at the centers of the faces. Though this trend appears in both HF and LDA, the details of the cluster structure are sensitive to the calculation method. Up to $N \leq 60$ the polymorphism, which is typical of the bulk state of silicon, leads to an explosive growth of the number of possible structures, often linked in families with a common mode of growth. Generally these clusters have a cage-like structure whose external rings are reminiscent of either fullerenes or crystalline silicon [7,18,19]. From the experimental side, ion mobility measurements (see [7,8,19] and references therein) indicate that up to the size $N = 35$ cation clusters track the prolate growth pattern also observed for germanium and tin. Above this size the clusters gradually rearrange themselves towards a nearly spherical geometry.

AM1 calculations for the size $N \leq 40$ are reported in Tables 1 and 2. In order to compare the calculations with the shapes reported in the literature, the clusters were structurally characterized on the basis of their average bond length R_b and of their aspect ratio, i.e. the ratio between the inertial moments calculated with respect to two in-plane equatorial axes. However the property more relevant in the context of this study is stability. In the cluster literature the parameters commonly adopted to describe this quantity are the binding energy E_b and the energy $E_e(m)$ required for the emission of a subunit of size m (thereafter indicated as emission energy). These

Table 1. Properties of silicon clusters. AM1 calculations and literature results E_b, R_b and I_p indicate the binding energy, the average bond length and the ionization potential, respectively. The source of references for $N \leq 10$, $N = 23$ and $N = 28$ is [17–19], respectively.

literature results: experiment				
cluster	structure	E_b (eV/atom)	I_p (eV)	R_b (Å)
Si_2	-	–1.61	7.40	-
Si_3	-	–2.56	-	-
literature results: theory				
cluster	structure	E_b	I_p	R_b
Si_2		–1.58	7.50	2.23
Si_3	isosceles triangle	–2.56	7.90	2.43
Si_4	rhombus	–3.31	7.60	∼2.35
Si_{10}	C_{3v}	–4.32(–3.92)	-	-
Si_{23}		–3.75		
Si_{28}		–3.98		∼2.40
AM1 calculations				
cluster	structure	E_b (eV/atom)	I_p (eV)	R_b (Å)
Si_2		–1.46	8.60	2.28
Si_3		–2.79	8.30	2.27
Si_4		–3.15	8.30	2.10
Si_{10}	-	–3.66	7.39	2.44
Si_{23}	-	–4.15	7.14	2.64
Si_{28}	-	–4.15	7.11	2.39
Si_{36}	-	–4.25	7.63	2.36

energies can be obtained from the cluster energy E, evaluated from the stationary minimum, according to

$$E_b = (E(N) - NE_{\mathrm{Si}})/N$$
$$E_e(m) = E(N) - E(N-m) - E(m) \qquad (2)$$

where $E(N)$ is the total energy in the cluster of size N and E_{Si} is the energy of the free atom.

Structural parameters and binding and emission energies (absolute values) for $m = 1, 2$ are reported in Tables 1 and 2. For $N \leq 10$ the more common structural patterns (i.e. triangle, rhombus, and polytetrahedal) were found together with other structures of a linear, cyclic, or mixed polytetrahedal and cyclic, shape. The aspect ratio at $N = 36$ indicates the occurrence of prolate structures at N in the range 30. The size dependence of E_b shows a progression towards the bulk value while the parallel decrease of I_p suggests a distributed and/or delocalized charge. As for E_b, the size dependence of E_e indicates an increased stability with the increase of the cluster size.

Table 2. Properties of silicon clusters. AM1 calculations. $E_e(1)$, $E_e(2)$ and E_e(dimer) indicate the energy needed for the emission of one, two monomers or one dimer, respectively.

properties of fragmentation					
cluster	E_b (eV/atom)	aspect ratio	$E_e(1)$ (eV)	$E_e(2)$ (eV)	E_e(dimer) (eV)
Si_{10}	–3.66	1.25	4.37	7.61	1.95
Si_{23}	–4.15	1.26	5.78	8.47	2.80
Si_{28}	–4.15	2.54	6.22	10.6	7.65
Si_{36}	–4.25	2.00	4.73	9.82	4.16

Furthermore the comparison of the values of E_e for emission into the channel of monomers and dimers shows that the emission of a subcluster of size m is energetically favored over the one of m monomers. This is not counterintuitive as the first of these channels does not require the additional energy of m separate fragmentation processes.

To conclude this section, it is underlined that the limited comparison performed in Table 1 indicates a constant trend towards overbinding at the larger sizes. Quantitatively, the divergences with respect to literature data fall in the range 10–15%. These results are encouraging if one considers that a parametrized Hamiltonian is a rather unrefined approach. In addition, the study of fragmentation showed that the cluster evolution is chiefly determined by the cluster size rather than by the details of its structural properties. Therefore an inaccurate evaluation of the ground state is of scarce significance in the context of this work.

4 Fragmentation

Literature results offer some hints on general properties of fragmentation. Studies on rare-gas, alkaline and noble metals and fullerenes indicate that for E_k noticeably lower than the bulk melting temperature the cluster acquires a roto-vibrational energy and its shape oscillates between structures with a remarkably different shape. This stage does not imply a considerable alteration of E_b. However the increase of E_k generates structures with a lower binding strength and promotes fragmentation. The fragmentation channels have a complex dependence on the element forming the cluster, on the cluster size and on the technique adopted to obtain fragmentation. Systematic studies on these parameters are scarce and a general remark is that fragmentation, as all dynamical phenomena, is much less understood than its stationary counterparts. In the case of silicon early studies [1–4] showed that the most prominent species obtained from fragmentation of the ionized clusters Si_N^+, with N from 2 to 12, are Si_6^+ and Si_{10}^+. More recent results [5,6] indicate that this behavior extends up to $N = 100$ while nanometric clusters prevalently evaporate monomers and dimers. From a theoretical point of view, molecular dynamics simulations using the Car-Parrinello method show that clusters with $N \leq 12$ acquire a liquid-like structure when heated to a temperature of some tenths of eV [20].

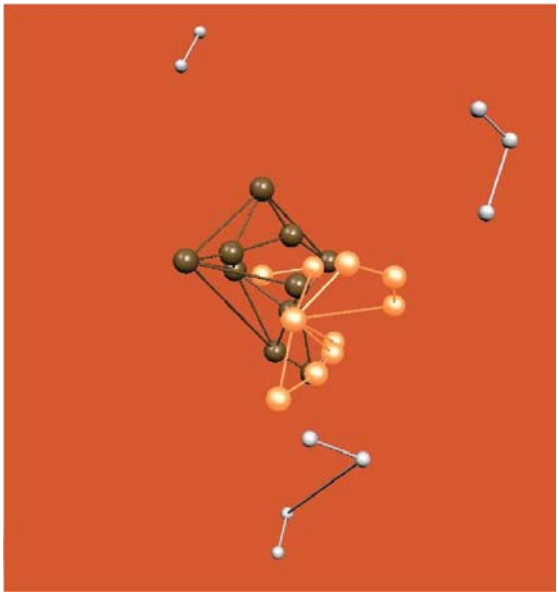

Fig. 1. The structure of Si_{10} for $t = 0$, 300 and 600 fs. E_k = 2.0 eV/atom. The darker spheres show the cluster ground state. The scattered dimers and trimers on the figure margins show the final stage of fragmentation.

The quantities addressed by the simulations are the evolution of the cluster shape and the minimum energy E_k required for fragmentation (thereafter indicated as Dynamical Fragmentation Energy, or DFE). For the evaluation of DFE two sets of calculations were made for each size. In the first series a large mesh of E_k values (steps around 0.2 and 0.5 eV/atom) was used to detect fragmentation. Afterwards, E_k was finely binned with a step of 0.05 eV/atom starting from the energy where fragmentation was first observed. Fragmentation was assumed to occur when some cluster atom was carried at a distance 3–4 Å larger than the maximum internuclear distance in the cluster ground state.

The calculations showed that fragmentation occurs with the mode of a liquid droplet [21]. Accordingly, the fragmentation transient consists on two stages, i.e. incubation and formation of fragments. During the first stage the potential and kinetic energy intraconvert and a substantial modification of the cluster shape derives from the lowering of its potential energy. Depending on the imbalance between kinetic and potential energy, a second stage follows during which the cluster acquires an even more fluxional shape till small fragments are carried at a perceptible distance from the original cluster body.

Illustrative examples of this evolution are given in Figures 1 and 2, which presents a 3D and a 2D view, respectively, of successive stages of fragmentation for the size $N = 10$. The view in Figure 1 shows the displacements and the deformation precursor of fragmentation (light circles) and the formation of scattered dimers and trimers at the completion of the process. In Figure 2 the transient is started with E_k below and above DFE (Figs. 2A and 2B, respectively). In these plots the lines are drawn to show the cluster perimeter and maximum size. Therefore there is no correspondence between these lines and bond lengths. This presentation shows an expansion of the original cluster shape according to an approximate Lissajous figure, which suggests repulsive interactions and ballistic motions. The effect is perceptibly larger at the higher E_k (Fig. 2B). In this case scattered groups of atoms, containing up to 5 atoms, are formed at $t \sim 600$ fs. In the figure the sites of these atoms are marked by the darker ellipses to underline the analogy with the separated, capillary waves formed by the evolution of a liquid droplet.

A noticeable feature of the fragmentation transient is its irregular evolution. For instance, in Figure 2 the amplitude of the cluster dilation in the time interval 500–600 fs is comparable to the one occurring in all its precedent history. Further evidence on this irregular behavior is offered by Figure 3, which shows the evolution of Si_{28} at $t = 500$ fs for $E_k = 0.15$ eV/atom. A considerable reshaping is observed even for this cluster which has a comparatively large size. A further interesting effect is the formation upon fragmentation, of a more compact, and therefore more robust, structure. This state is however metastable and decays in time or under the effect of a small additive input energy.

The calculations reported above resume the main features of fragmentation as observed in this study, i.e. the fragmented structures consist of a compact body surrounded by detached groups of atoms of size $N \leq 5$. At the smaller size (Fig. 1) the cluster is entirely dismembered into these small fragments. These results are limited to the duration of the simulations, i.e. approximately 1000 fs, and no attempt has been made to track reaggregation of the small subclusters among them or with the parent cluster. However two features were found to be common to all transients. In the first place, a constant characteristic of both the fragments and the parent cluster is a profound structural change with respect to the ground state. In the second place no obvious structural connection was found among fragments of size $N = 3,\ 4,\ 5$ and the shape of the stationary clusters of the same size.

The relationship between the characteristic energies, dynamical and stationary, is illustrated in Figure 4. In this figure the energies are normalized to E_b to make the connection with the cluster cohesion more transparent. The noticeable feature of these plots is the low value of DFE in comparison with the E_e, though the size dependence is generally similar. The physical ground underlying this effect is the deformation of the cluster connectivity and of its bonding mode during the transient. This leads to important changes of the barrier toward fragmentation with respect to its stationary evaluation.

As a concluding remark, though divergences with experiments are observed, also consistent results are found. This seems important, if one considers the complexity of QM time-dependent methods. In fact, the fragment sizes $N = 6,\ 10$ observed in experiments are not in contradiction with the fragmentation pattern described above. In the frame of our simulations these clusters would be either the remainings of the original clusters or the results of the reaggregation of smaller clusters formed by fragmentation.

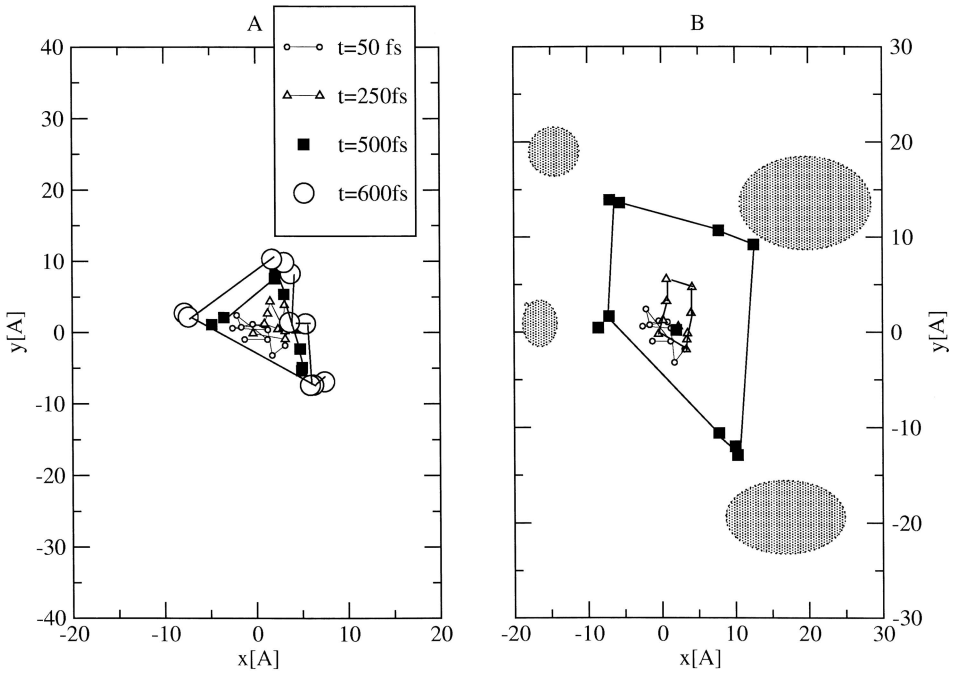

Fig. 2. Plane-view of the evolution of the clusters Si_{10} for the times shown. A: $E_k = 2.0$ eV/atom. B: $E_k = 7.0$ eV/atom.

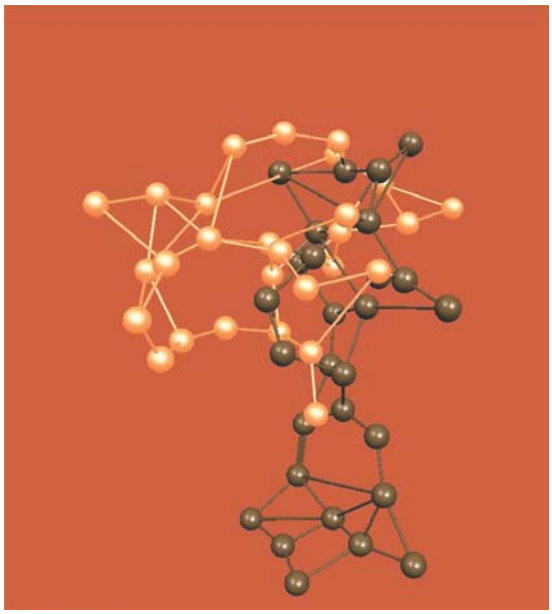

Fig. 3. Si_{28} at $t = 0$ and $t = 500$ fs for $E_k = 0.5$ eV/atom. The darker spheres show the cluster ground state.

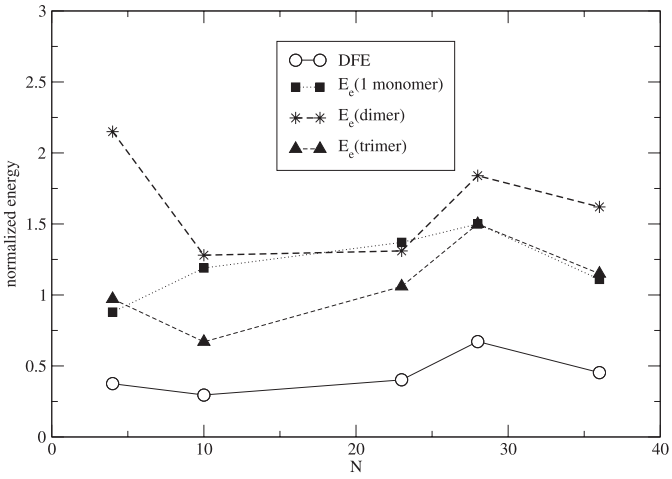

Fig. 4. The functional dependence of the emission energies and of DFE on size.

Furthermore the dissociation energy, deduced from fragmentation experiments, decreases from above 4 eV at $N = 10$ to 2.5 eV at $N = 20$ [7]. In agreement with the experimental asymptote at large size, the value of DFE at $N \geq 20$ is approximately equal to 2 eV (Fig. 4). However its value at small N is still in the range 1 eV and therefore considerably lower than the experimental one. As for the stationary energies reported in the previous section, this failure is attributed to the inadequacy of the AM1 parametrization of reconstructing subtle effects of the size on E_b. This does not invalidate the meaning of the results presented above.

5 Conclusions

In conclusion, this study shows the evolution of small silicon clusters under the effect of an external energy input. No claim is made that all possible channels of fragmentation have been identified. Polymorphism is a known property of clusters and it plagues fragmentation as any other property of these structures. Under the given fragmentation conditions, the simulations suggest the formation of fragments above the monomer size, which is in agreement with the experimental trend.

References

1. T.P. Martin, H. Schaber, J. Chem. Phys. **82**, 855 (1985)
2. L.A. Bloomfield, R.R. Freeman, W.L. Brown, Phys. Rev. Lett. **54**, 2246 (1985)
3. Q. Cheshnovsky et al., Chem. Phys. Lett. **138**, 119 (1987)
4. Q.L. Zhang, Y. Liu, R.F. Curl, F.K. Tittel, R.E. Smalley, J. Chem. Phys. **88**, 1670 (1988)
5. M.F. Jarrold, E.C. Honea, J. Chem. Phys. **95**, 9181 (1991)
6. M. Ehbrecht, F. Huisken, Phys. Rev. B **59**, 2975 (1999)
7. A.A. Shvartsburg, M.F. Jarrold, B. Liu, Z.-Y. Lu, C.Z. Wang, K.M. Ho, Phys. Rev. Lett. **81**, 4616 (1998)
8. A.A. Shvartsburg, B. Liu, Z.Y. Lu, C.Z. Wang, M.F. Jarrold, K.M. Ho, Phys. Rev. Lett. **83**, 2167 (1999)
9. A.M. Mazzone, Comp. Mat. Sci. **18**, 185 (2000)
10. M.J. Field, J. Chem. Phys. **96**, 4583 (1992)
11. J. Jellinek, D.H. Li, Chem. Phys. Lett. **169**, 380 (1990)
12. A.J. Stace, J. Chem. Phys. **93**, 6502 (1990)
13. Quantum Chemistry Program Exchange: Program Number 571 and references therein. Information on QCPE can be found at the web site `www.indiana.edu`
14. M.J.S. Dewar, W. Thiel, J. Am. Chem. Soc. 4899 (1977)
15. J.P. Stewart, J. Comput. Chem. **10**, 209 (1989)
16. J.D. Thompson, C.J. Cramer, D.G. Truhlar, J. Comp. Chem. **24**, 1291 (2003)
17. K. Ragachavari, C.M. Rohlfing, J. Chem. Phys. **89**, 2219 (1988)
18. I. Rata, A.A. Shvartsburg, M. Hiroi, T. Fraunenheim, K.W.M. Siu, K.J. Jackson, Phys. Rev. Lett. **546**, 85 (2000)
19. X.G. Gong, Phys. Rev. B. **52**, 14677 (1995)
20. Z.Y. Lu, C.Z. Wang, K.M. Ho, Phys. Rev. B **61**, 2329 (2000)
21. G. Guet, X. Biquard, P. Blaise, S.A. Blundell, M. Gross, B.A. Huber, D. Jalabert, M. Maurel, L. Plagne, J.C. Rocco, Z. Phys. D **40**, 317 (1997)